

## INVESTIGATION OF GAMOW-TELLER STRENGTHS FOR A=34 AND A=37 NUCLEI

Malik S. Mehemed<sup>1</sup>, Sarah M. Obaid<sup>2</sup>, Fouad A. Majeed<sup>3</sup>

<sup>1</sup>Education Directorate Babylon, Ministry of Education, Babil, Iraq;

<sup>2</sup>Technical College of Al-Mussaib, Al-Furat Al-Awsat Technical University, Babylon, Iraq;

<sup>3</sup>Department of Physics, College of Education for Pure Sciences University of Babylon, Babylon, Iraq

E-mail: fmajeed@uobabylon.edu.iq

In this work, the Gamow-Teller transition strength distributions in *sd*-shell region were investigated by using shell model. The calculations of B(GT) and their accumulated sum  $\sum B(GT)$  for the nuclei  $^{34}\text{Ar} \rightarrow ^{34}\text{Cl}$ ,  $^{34}\text{S} \rightarrow ^{34}\text{Cl}$ ,  $^{37}\text{Cl} \rightarrow ^{37}\text{Ar}$ , and  $^{37}\text{Ca} \rightarrow ^{37}\text{K}$  were performed using the shell model by utilizing the USDB and USDA effective interactions in the *sd*-shell. The transitions for the nuclei are studied. The results for the B(GT) and  $\sum B(GT)$  are discussed and compared to the most recent observed data. The measured GT distributions and the cumulative transition intensities B(GT) are in a fair amount of agreement with the theoretical calculations. We have established a qualitative agreement for the individual transformations, and the measured cumulative transformation strengths nearly match the observed ones.

PACS: 21.60.Cs, 26.50.+x, 23.40.-s, 25.40.Kv

### INTRODUCTION

The spin isospin ( $\sigma\tau$ ) interaction mediates Gamow-Teller (GT) transitions. The transfer of the angular momentum ( $\Delta L=0$ ) and the exchange of spin-isospin ( $\Delta S=1$  and  $\Delta T=1$ ) are used to identify the transitions. Due to their straightforward nature, GT transitions are important tools for the study of nuclear structure [1 - 5]. Additionally, they control the majority of nuclear weak-interaction activities during nucleosynthesis [6]. Experimental research on GT transitions focuses on both charge-exchange (CE) processes and decays. Although the Q values and the partial half-lives may be used to evaluate decays' direct access to the B(GT) strength, there are only a few transitions that can be achieved. Contrarily, the CE reactions are capable of selectively activating GT states at high excitation energy [7]. However, Adelberger and Haxton [8] discovered substantial disparities between the  $^{37}\text{Cl}$  ( $p, n$ )  $^{37}\text{Ar}$  and the  $^{37}\text{Ca}$   $\beta$ -decay data some years later. The investigation of isospin symmetry might benefit from high-resolution measurements of GT transitions [9]. When comparing the GT transition intensities produced by  $\beta$ -decays to those achieved by ( $^3\text{He}, t$ ) reactions for odd-mass nuclei, the  $T_z = \pm 1/2$  the low-lying spectra of nuclei in the *sd*-shell has been investigated for isospin symmetry [10 - 12]. Similar to that, researchers have looked at the transitions of GT for the symmetry of the isospin from the  $T_z = \pm 1$  nucleus to the  $T_z = 0$  nucleus for some of the studied isobars that lies in the *sd*-shell, for example the nuclei with mass number  $A=26$  ( $^{26}\text{Mg}$ ,  $^{26}\text{Al}$ , and  $^{26}\text{Si}$ ) [13] or  $A=34$  ( $^{34}\text{S}$ ,  $^{34}\text{Cl}$ , and  $^{34}\text{Ar}$ ) [13]. For the four strong variables, there were a satisfactory B(GT) values that match with a difference of no more than 5% for  $T_z = \pm 1 \rightarrow 0$  GT transitions in the  $A = 26$  system. It indicated that a reasonable scattering angle for the isospin symmetry existed. Previously the GT strengths and their accumulated sum were calculated and compared with the measured data for *sd*- and *fp*-shell nuclei in which the B(GT) values agreed reasonably well [14 - 17].

The purpose of this study is to calculate the B(GT) strength distribution for the *sd*-shell selected nuclei. Theoretical shell model calculations were conducted by using the NushellX@MSU [18] shell model code to calculate the distributions B(GT) strengths for  $^{34}\text{Ar} \rightarrow ^{34}\text{Cl}$ ,  $^{34}\text{S} \rightarrow ^{34}\text{Cl}$ ,  $^{37}\text{Cl} \rightarrow ^{37}\text{Ar}$ , and  $^{37}\text{Ca} \rightarrow ^{37}\text{K}$  in the *sd*-shell by utilizing the effective interactions USDA and USDB that is best fitted for the *sd*-shell mass region. The obtained values of B(GT) and their B(GT) cumulative values will be compared to the measured data and a conclusion of this study will be drawn.

### 1. THEORETICAL BACKGROUND

Nuclear beta decay research reveals details regarding the nature of the weak interaction as well as the structure of nuclear wave functions. The electron and neutrino's angular momenta can be used to classify beta decay. The most significant momentum which have ( $\Delta \ell = 0$ ) is known as allowed beta decay. The beta decay of Fermi and Gamow-Teller are two types of permitted beta decay. The operator linking the initial and final states to the GT transition may be represented as [19, 20].

$$\langle \sigma\tau \rangle = \frac{\langle f \left| \sum_k \sigma^k \tau_{\pm}^k \right| i \rangle}{\sqrt{2J_i + 1}}, \quad (1)$$

with

$$\tau_{\pm} = \frac{1}{2} (\tau_x + i\tau_y), \quad (2)$$

where  $\sigma$  is the Pauli operator and  $\tau$  is the isospin operator;  $|f\rangle$  is the final and  $|i\rangle$  is the initial states for transition, respectively.

The B(GT) is a widely used measure of the strength of GT and is the probability reduction for the transition from GT [19].

$$B(GT) = \left( \frac{g_A}{g_V} \right)^2 \langle \sigma\tau \rangle^2, \quad (3)$$

where the ratio of the vector axial of the constants to the coupling vector is  $|g_A/g_V|=1.26$ . The sum rule is as follows for the GT reduced elements matrix [19].

$$\sum_f [B_{i,f}(GT_-) - B_{i,f}(GT_+)] = 3 \left( \frac{g_A}{g_V} \right)^2 (N_i - Z_i). \quad (4)$$

## 2. RESULTS AND DISCUSSIONS

The summed B(GT) values are reviewed and contrasted with the actual data in this part along with the anticipated values of the strengths of B(GT). The NusheX@MSU is the code used to perform all calculations [18].

### 2.1. $^{34}\text{Ar} \rightarrow ^{34}\text{Cl}$

The strengths transition of B(GT) as a result of the change from the  $^{34}\text{Ar}(0^+)$  ground state to  $^{34}\text{Cl}(1^+)$  states calculated using shell model with the effective interactions USDB and USDA is depicted in Fig. 1. The observed data for distribution of B(GT) strengths in  $^{34}\text{Cl}(\beta^+)$  are measured to the excitation energy for the energies below 5.751 MeV [21]. The experiment's two most significant peaks are situated at  $E_x(^{34}\text{Cl}) = 2.58$  and 3.129 MeV with values of B(GT) 1.36 and 1.399, respectively. The transitions produce these two peaks comes from the transition  $^{34}\text{A}(0^+) \rightarrow ^{34}\text{Cl}(1_4^+)$  and  $(1_5^+)$ , respectively. The analysis for USDA and USDB interactions revealed three high peaks at 1.989, 2.884, and 4.568 MeV with the values of B(GT) as 0.418, 1.704 and 1.516, respectively. Two dominant peaks appeared from the calculations of USDA interactions comes from  $^{34}\text{A}(0^+) \rightarrow ^{34}\text{Cl}(1_3^+)$ ,  $(1_4^+)$ , and  $(1_7^+)$ , respectively.

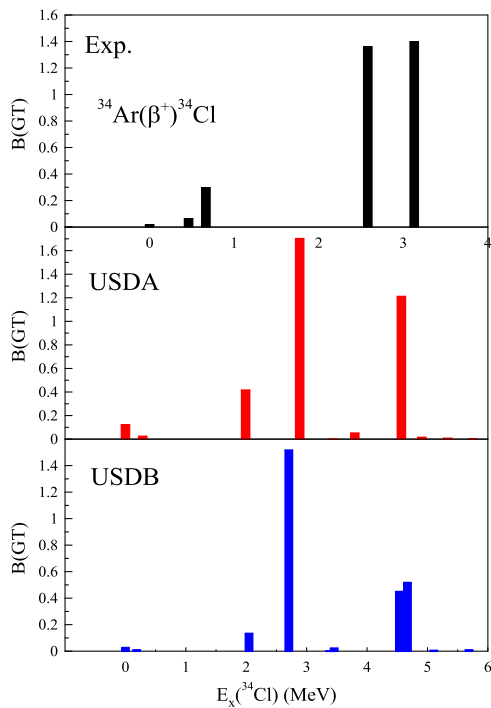


Fig. 1. Comparison of the predicted values of  $B(GT)$  for the  $^{34}\text{Ar} \rightarrow ^{34}\text{Cl}$  transition with the relevant measured data [21]

The USDB interaction shows three strong peaks situated at 2.705, 4.535, and 4.669 MeV which correspond to the values of B(GT) 1.516, 0.449, and 0.517, respectively, that comes from  $^{34}\text{A}(0^+) \rightarrow ^{34}\text{Cl}(1_4^+)$ ,  $(1_7^+)$ , and

$(1_8^+)$  transitions, respectively. The cumulative total of  $B(GT)$  is shown in relation to the excited energy in Fig. 2. Theoretical computations utilizing the effective interactions for the shell model show that the estimated  $B(GT)$  and the summed values of the  $B(GT)$  reproduced by USDB and USDA interactions closely match the data.

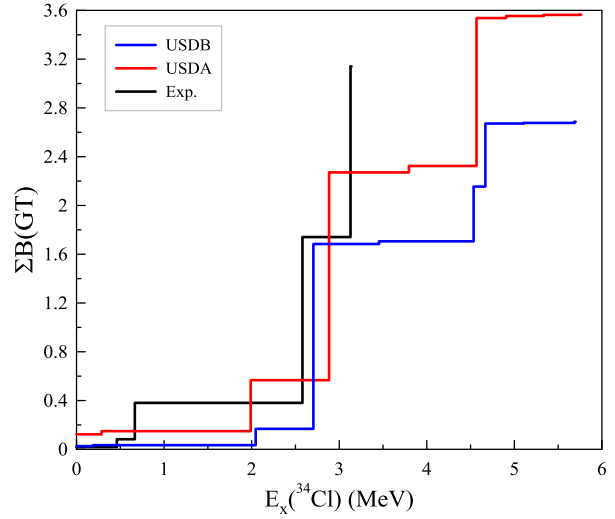


Fig. 2. Comparison of  $\Sigma B(GT)$  distribution to the measured data [21] for  $^{34}\text{Ar} \rightarrow ^{34}\text{Cl}$  transition

### 2.2. $^{34}\text{S} \rightarrow ^{34}\text{Cl}$

Fig. 3 displays experimental data for the  $^{34}\text{S} \rightarrow ^{34}\text{Cl}$  transition GT strengths along with the shell model prediction. Using USDA and USDB interactions, the values of B(GT) were predicted from the transition of the ground state of  $^{34}\text{S}(0^+)$  to  $^{34}\text{Cl}(1^+)$  states).

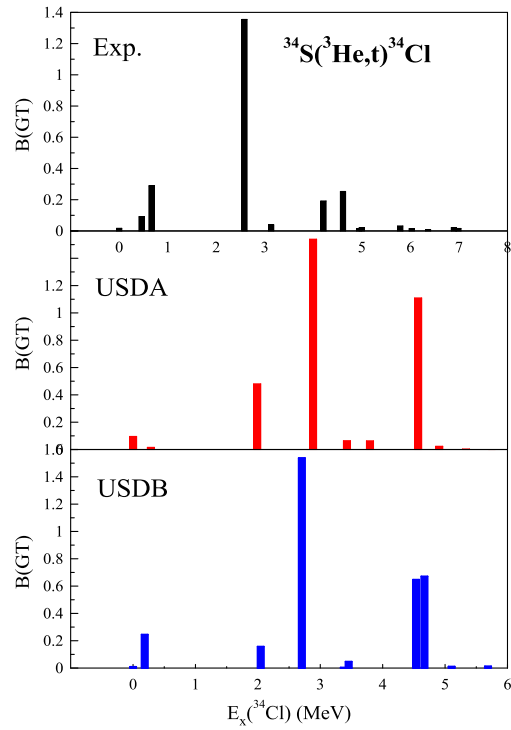


Fig. 3. Comparison of the predicted values of  $B(GT)$  for the  $^{34}\text{S} \rightarrow ^{34}\text{Cl}$  transition with the relevant measured data [21]

The observed data measured from the charge exchange reaction  $^{34}\text{S}(\text{He}, \text{t})^{34}\text{Cl}$  [22]. The highest value

seen in the measured data for  $^{34}\text{S}(^{34}\text{He}, \text{t})^{34}\text{Cl}$  reaction is situated at  $E_x(^{34}\text{Cl})=2.581$  MeV with  $B(\text{GT})$  value 1.355. Theoretical estimates utilizing USDA interaction show three significant peaks at  $E_x(^{34}\text{Cl}) = 1.989, 2.884$ , and 4.568 MeV while the predicted USDB three strong peaks located at  $E_x(^{34}\text{Cl}) = 2.705, 4.535$ , and 4.669 MeV. The cumulative total of the values of  $B(\text{GT})$  estimated by USDB and USDA are compared with the observed data in Fig. 4. The results of the USDA and USDB agree reasonably well till the excitation energy 4.5 MeV and starts overestimate the accumulated values of the  $B(\text{GT})$ .

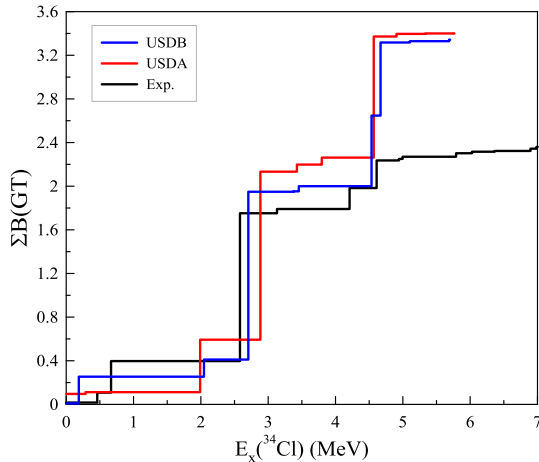


Fig. 4. Comparison of the  $\Sigma B(\text{GT})$  distribution with the measured data [21] for  $^{34}\text{S} \rightarrow ^{34}\text{Cl}$  transition

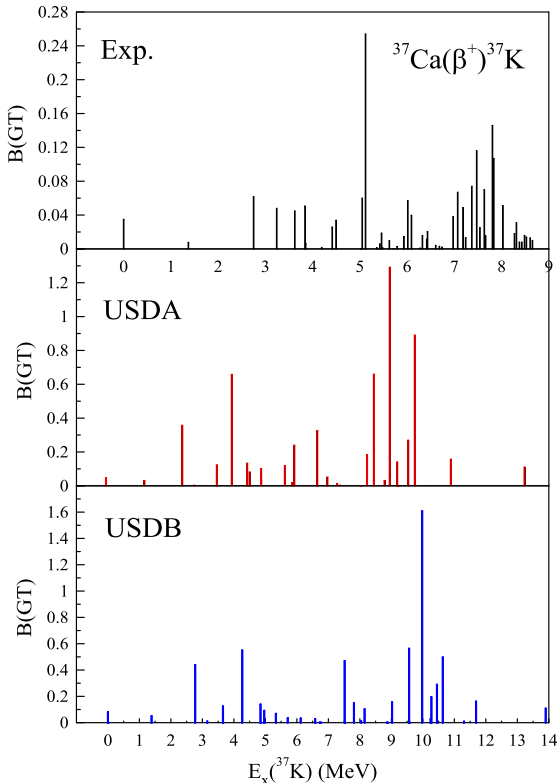


Fig. 5. Comparison of the predicted values of  $B(\text{GT})$  for the  $^{37}\text{Ca} \rightarrow ^{37}\text{K}$  transition with the relevant measured data [22]

### 2.3. $^{37}\text{Ca} \rightarrow ^{37}\text{K}$

Fig. 5 illustrated the comparison of the calculated values of  $B(\text{GT})$  using the shell model space  $sd$  with the

measured data for the transition  $^{37}\text{Ca} \rightarrow ^{37}\text{K}$ . Predictions of the  $B(\text{GT})$  values start at the lowest level of  $^{37}\text{Ca}$  ( $3/2^+$ ) to  $^{37}\text{K}$  ( $1/2^+, 3/2^+, 5/2^+$ ) levels using the USDA and USDB interactions. The observed experimental data for  $^{37}\text{Ca} \rightarrow ^{37}\text{K}$  comes from the Charge-exchange reaction via  $^{37}\text{Ca}(\beta^+)^{37}\text{K}$  [22]. The highest peak appear in observed data is situated at  $E_x(^{37}\text{K})=5.12$  MeV which corresponds to  $B(\text{GT})$  value 0.254. The ground-state is correctly predicted for  $^{37}\text{Ca}$  and  $^{37}\text{K}$  nuclei as ( $3/2^+$ ) utilizing USDB and USDA interactions. There are forty predicted values of  $B(\text{GT})$  that result from transitions  $^{37}\text{Ca}$  ( $3/2^+$ ) to  $^{37}\text{K}$  ( $1/2^+, 3/2^+, 5/2^+$ ), twelve of them are zero values, five are the highest values and the rest twenty-three are very low values predicted by both USDB and USDA interactions. Fig. 6 compares the total summed  $B(\text{GT})$  values which is predicted by the shell model calculations and it shows clearly the data values very weak compared to theory and the last value is around 8.6 MeV, while theory predicts higher values of  $B(\text{GT})$  that reach to around  $\approx 14$  MeV.

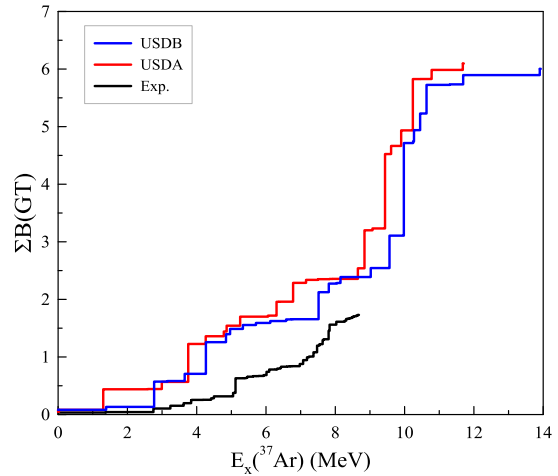


Fig. 6. Comparison of the  $\Sigma B(\text{GT})$  distribution with the measured data [22] for  $^{37}\text{Ca} \rightarrow ^{37}\text{K}$  transition

### 2.4. $^{37}\text{Cl} \rightarrow ^{37}\text{Ar}$

Fig. 7 illustrates the observed and calculated strengths of the  $B(\text{GT})$  transition from the  $^{37}\text{Cl}$  ( $3/2^+$ ) lowest state to the  $^{37}\text{Ar}$  ( $1/2^+, 3/2^+, 5/2^+$ ) states without any limitation utilizing the USDA and USDB effective interactions. The range of the excitation energy from 0 to 14.192 MeV and the strength of  $B(\text{GT})$  distribution comes from the measured data of the charge-exchange reaction  $^{37}\text{Ar} (^3\text{He}, \text{t}) ^{37}\text{Ar}$  [22]. The experiment's several main peaks are distributed between  $E_x(^{37}\text{Ar})=5.1$  and 9.35 MeV which corresponds to the values of  $B(\text{GT})$  at 0.226 and 0.117, respectively. The USDA interaction shows many peaks and the strongest two peaks were situated at 9.61 and 9.978 MeV which corresponds to the values of  $B(\text{GT})$  at 1.292 and 1.608, respectively. The USDB interaction predicts also some peaks and the strongest one situated at 9.61 MeV with  $B(\text{GT})$  value of 1.292 which is related to the transition  $^{37}\text{Cl}(3/2^+) \rightarrow ^{37}\text{Ar}(5/2_7^+)$ . The USDB interaction predicts 40  $B(\text{GT})$  values and the most highest peak situated at 9.978 MeV with  $B(\text{GT})$  of 1.608 which comes from the transition  $^{37}\text{Cl}(3/2^+) \rightarrow ^{37}\text{Ar}(5/2_7^+)$ . Fig. 8 depicts the comparison between the theoretical and measured summing of the  $B(\text{GT})$  as a function of the excitation energy.

The  $B(GT)$  summation strength is seen up to 14.19 MeV of excitation energy. The predicted values of  $B(GT)$  from theory gives more higher values that appear in their sum and therefore they overestimated the observed data.

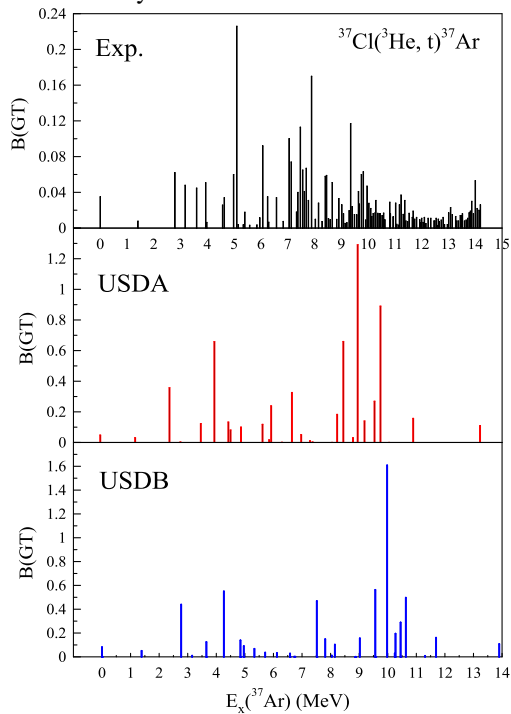


Fig. 7. Comparison of the predicted values of  $B(GT)$  for the  $^{37}\text{Cl} \rightarrow ^{37}\text{Ar}$  transition with the relevant measured data [22]

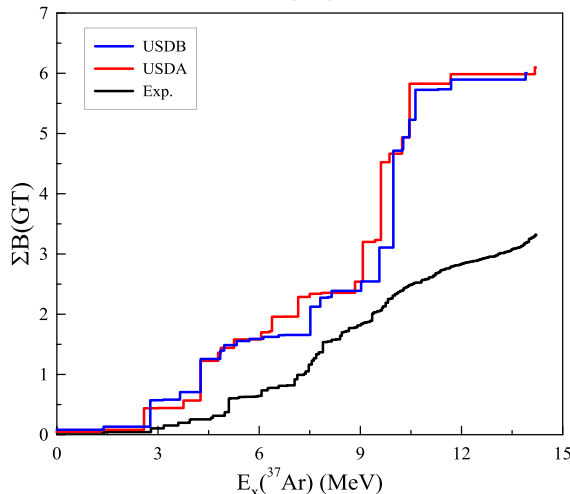


Fig. 8. Comparison of the  $\Sigma B(GT)$  distribution with the measured data [22] for  $^{37}\text{Cl} \rightarrow ^{37}\text{Ar}$  transition

## CONCLUSIONS

To investigate the GT strengths, we have presented the calculations utilizing the shell model in the complete  $sd$ -shell model space utilizing USDA and USDB interactions without valence nucleon truncation for the  $^{34}\text{Ar} \rightarrow ^{34}\text{Cl}$ ,  $^{34}\text{S} \rightarrow ^{34}\text{Cl}$ ,  $^{37}\text{Cl} \rightarrow ^{37}\text{Ar}$ , and  $^{37}\text{Ca} \rightarrow ^{37}\text{K}$  transitions. The used effective interactions in this work show clearly, they are able to predict the  $B(GT)$  values and they are in reasonable agreement with the measured data. Our research contributes to previous studies on GT strength distributions. The  $B(GT)$  transitions on an individual basis have attained satisfactory agreement, whereas the estimated strengths of the transition total

approximately reproduce the observed data. This result may be useful for future research into the transition strengths  $B(GT)$ .

## REFERENCES

1. A. Bohr and B.R. Mottelson. *Nuclear Structure* / 1st ed. v. 1 Benjamin, New York, 1969, p. 345-353.
2. F. Osterfeld. Nuclear spin and isospin excitations // *Reviews of Modern Physics* (64). 1992, p. 491-557.
3. B. Rubio and W. Gelletly. Beta Decay of Exotic Nuclei // *Lecture Notes in Physics* (764). 2009, p. 99-151.
4. J. Rapaport and E. Sugarbaker. Isovector excitations in nuclei // *Annual Review of Nuclear and Particle Science* (44). 1994, p. 109-153.
5. Y. Fujita, B. Rubio, and W. Gelletly. Spin-isospin excitations probed by strong, weak and electromagnetic interactions // *Progress in Particle and Nuclear Physics* (66). 2011, p. 549-606.
6. K. Langanke and G. Martínez-Pinedo. Nuclear weak-interaction processes in stars // *Reviews of Modern Physics* (75). 2003, p. 819-862.
7. T. Taddeucci, C. Goulding, T. Carey, R. Byrd, C. Goodman, C. Gaarde, J. Larsen, D. Horen, J. Rapaport, and E. Sugarbaker. The  $(p, n)$  reaction as a probe of beta decay strength // *Nuclear Physics A* (469). 1987, p. 125-172.
8. E.G. Adelberger and W.C. Haxton.  $^{37}\text{Cl}$  solar neutrino capture cross section // *Physical Review C* (36). 1987, p. 879.
9. Y. Fujita, H. Akimune, I. Daito, H. Fujimura, M. Fujiwara, M.N. Harakeh, T. Inomata, J. Jänecke, K. Katori, A. Tamii, and M. Tanaka. Mirror-symmetry structure of  $A=27$ ,  $T=1/2$  nuclei studied through strong, weak, and electromagnetic interactions // *Physical Review C* (59). 1999, № 1, p. 90.
10. Y. Fujita, Y. Shimbara, A.F. Lisetskiy, T. Adachi, G.P.A. Berg, P. Von Brentano, H. Fujimura, H. Fujita, K. Hatanaka, J. Kamiya, and T. Kawabata. Analogous Gamow-Teller and M 1 transitions in  $^{26}\text{Mg}$ ,  $^{26}\text{Al}$ , and  $^{26}\text{Si}$  // *Physical Review C* (67). 2003, № 6, p. 064312.
11. R.G.T. Zegers, H. Akimune, S.M. Austin, D. Bazin, A.M. Van den Berg, G.P.A. Berg, B.A. Brown, J. Brown, A.L. Cole, I. Daito, and Y. Fujita. The  $(t, ^3\text{He})$  and  $(^3\text{He}, t)$  reactions as probes of Gamow-Teller strength // *Physical Review C* (74). 2006, № 2, p. 024309.
12. Y. Shimbara, Y. Fujita, T. Adachi, G.P.A. Berg, H. Fujita, K. Fujita, I. Hamamoto, K. Hatanaka, J. Kamiya, K. Nakanishi, and Y. Sakemi. Suppression of Gamow-Teller and M1 transitions in deformed mirror nuclei  $^{25}\text{Mg}$  and  $^{25}\text{Al}$ : Direct observation of K selection rules // *The European Physical Journal A-Hadrons and Nuclei* (19). 2004, № 1, p. 25-31.
13. Y. Fujita, R. Neveling, H. Fujita, T. Adachi, N.T. Botha, K. Hatanaka, T. Kaneda, H. Matsubara, K. Nakanishi, Y. Sakemi, and Y. Shimizu. Gamow-Teller strengths in  $A=34$  isobars: Comparison of the mirror transitions  $T_z=+1 \rightarrow 0$  and  $T_z=-1 \rightarrow 0$  // *Physical Review C* (75). 2007, № 5, p. 057305.

14. S.M. Obaid and H.M. Tawfeek. Gamow-Teller strengths of some sd-shell nuclei in the shell model framework // *Revista mexicana de fisica* (66). 2020, № 3, p. 330-335.
15. S.M. Obaid and H.M. Tawfeek. Investigation of strengths distributions of Gamow-Teller in sd- and fp-shell nuclei // *In IOP Conference Series ‘Materials Science and Engineering’* (871). 2020, № 1, p. 012086.
16. F.A. Majeed and S.M. Obaid. Calculations of Gamow-Teller Transition Strengths in fp-Shell Nuclei Using Shell Model // *Canadian Journal of Physics* (99). 2021, № 1, p. 33-37.
17. S.M. Obaid, F.A. Majeed, and F.E. Mohammed. Nuclear structure and Gamow-Teller B(GT) transition strengths for some selected fp-shell Nuclei // *Karbala International Journal of Modern Science* (8). 2022, № 3, p. 522-530.
18. B.A. Brown and W.D.M. Rae. The shell-model code NuShellX@ MSU // *Nuclear Data Sheets* (120). 2014, p. 115-118.
19. W.T. Chou, E.K. Warburton, and B.A. Brown. Gamow-Teller beta-decay rates for  $A \leq 18$  nuclei // *Physical Review C* (47). 1993, № 1, p. 163.
20. P.M. Endt. Energy levels of  $A = 21-44$  nuclei (VII) // *Nuclear Physics A* (521). 1990, p. 1-400.
21. N.T. Khai, B.D. Linh, T.D. Thiép, Y. Fujita, T. Adachi, H. Fujita, and A. Tamii. Determination of GT-transition Strengths in  $A=34$  Isobars using Charge Exchange ( $^3\text{He}, t$ ) Reaction // *Communications in Physics* (22). 2012, № 1, p. 91-96.
22. Y. Shimbara, Y. Fujita, T. Adachi, G.P.A. Berg, H. Fujimura, H. Fujita, K. Fujita, K. Hara, K.Y. Hara, K. Hatanaka, and J. Kamiya. High-resolution study of Gamow-Teller transitions with the  $^{37}\text{Cl}$  ( $^3\text{He}, t$ )  $^{37}\text{Ar}$  reaction // *Physical Review C* (86). 2012, № 2, p. 024312.

Article received 10.10.2023

## ДОСЛІДЖЕННЯ СИЛ ПЕРЕХОДУ ГАМОВА-ТЕЛЛЕРА ДЛЯ ЯДЕР $A=34$ І $A=37$

*Malik S. Mehemed, Sarah M. Obaid, Fouad A. Majeed*

Були досліджені розподілі сил переходу Гамова-Теллера в області *sd*-оболонки за допомогою моделі оболонки. Розрахунки B(GT) та їх накопиченої суми  $\sum B(GT)$  для ядер  $^{34}\text{Ar} \rightarrow ^{34}\text{Cl}$ ,  $^{34}\text{S} \rightarrow ^{34}\text{Cl}$ ,  $^{37}\text{Cl} \rightarrow ^{37}\text{Ar}$  та  $^{37}\text{Ca} \rightarrow ^{37}\text{K}$  виконано за допомогою оболонкової моделі з використанням ефективних взаємодій USDB та USDA у *sd*-оболонці. Досліджено переходи для ядер. Результати для B(GT) і  $\sum B(GT)$  обговорюються та порівнюються з даними останніх спостережень. Вимірюні розподілі GT та кумулятивні інтенсивності переходу B(GT) досить добре узгоджуються з теоретичними розрахунками. Встановлено якісну відповідність для окремих трансформацій, і вимірюні кумулятивні сили трансформації майже збігаються зі спостережуваними.